P H Y S I C A L   R E V I E W   L E T T E R S

Quantum Scattering of Fast Atoms and Molecules on Surfaces

P. Rousseau, H. Khemliche, A. G. Borisov, and P. Roncin*

CNRS, Laboratoire des Collisions Atomiques et Moléculaires, UMR 8625, Université Paris-Sud, Orsay, F-91405, France
(Received 3 October 2006; published 5 January 2007)

We present evidence for the diffraction of light keV atoms and molecules grazingly scattered on LiF(001) and NaCl(001) surfaces. At such energies, the de Broglie wavelength is 2 orders of magnitude smaller that the mean thermal atomic displacement in the crystal. Thus, no coherent scattering was expected and interaction of keV atoms with surfaces is routinely treated with classical mechanics. We show here that well-defined diffraction patterns can be observed indicating that, for grazing scattering, the pertinent wavelength is that associated with the slow motion perpendicular to the surface. The experimental data are well reproduced by an *ab initio* calculation.

In 1930 the report by Estermann and Stern [1] of diffraction of He atoms and H_2 molecules on a NaCl crystal played a key role in establishing the main concept of quantum mechanics, namely, the particle-wave dualism. Since then, thermal energy atom scattering (TEAS) has become a very powerful diffraction technique. Applied to surface science it is used to derive surface specific properties such as crystallographic parameters but also adsorbate mobility [2], and phonon dispersion properties [3]. Similarly, diffraction of low-energy electrons, in the 100 eV range (LEED) [4], is routinely used in surface science. In both cases, the de Broglie wavelengths of the projectiles are comparable to lattice constants. Similar to light scattering on gratings or x-ray scattering on crystals, diffraction on periodic systems results in structured patterns that reflect the exchange of reciprocal lattice vector(s) between the incident wave and the periodic structure.

The continuous progress of laser cooling techniques have brought atoms below nano Kelvin temperatures with wavelengths over the micron range. At this level, the surface atomic structure is not visible and new quantum phenomena such as long range reflection on the attractive Casimir-Polder potential are observed [5]. These mesoscopic wavelengths have allowed, for instance, the observation of Bose-Einstein condensate and have boosted the advent of atom optics [6,7].

As for atomic collisions at surfaces in the keV regime, diffraction was not believed to be observable. Indeed, the de Broglie wavelength $\lambda < $ pm of keV projectiles is much smaller than the mean thermal displacement of the surface atoms so that buildup of coherence seems unlikely. Moreover, for, e.g., metallic surfaces, the electronic excitations resulting in the projectile stopping would progressively break the coherence. Therefore, classical projectile trajectory approximation has been routinely used to explain results of extensive experimental studies of fast atomic collisions with surfaces [8,9]. Presently, classical-trajectory-based computer codes are available that cover wide range of phenomena (sputtering, scattering, energy loss) [10] and quantum-mechanics is usually evoked only to treat the electronic processes.

In this Letter we show that well-defined diffraction patterns can be observed with keV projectiles in surface scattering experiments. A mandatory condition is the grazing scattering geometry where the projectile is reflected by the topmost surface layer, and the dynamics of the projectile-surface interaction is characterized by the slow (fast) motion perpendicular (parallel) to the surface [9]. A favorable condition is to direct the incident beam along a low index direction of the target crystal. The successive surface atoms that scatter the projectile are then aligned, forming rows that can temporarily guide the projectile resulting in a well-known classical rainbow in the scattering profile [11,12]. Finally, one would like to quench the electronic excitations in the surface to avoid subsequent decoherence. In this respect, wide band gap insulators, such as ionic crystals used here, represent then an ideal choice [9,13].

In the present experiment an ion beam of the desired energy is mass selected and sent through a gaseous charge exchange cell to produce a neutral beam. Its divergence is reduced to the mrad range with two 0.1 mm diaphragms 0.5 m apart. The single crystal surface of LiF(001) or NaCl(001) is placed on a manipulator in a UHV chamber and maintained at room temperature. It is oriented *in situ* along a crystallographic axis with an electron diffraction system. After collision at typical incidence angles θ of the order of 1 deg the reflected beam is collected on a 40 mm wide microchannel plate position sensitive detector located 0.6 m downstream. In the following we will use the Cartesian coordinates with z axis normal to the surface and pointing into the vacuum, x (y) axis is in the surface plane along (perpendicular) to the direction of the incident beam. For calibration purpose, the target is not fully inserted in the incident beam so that some projectiles reach the detector without any interaction with the surface. One can then define a center point $C(y = 0, z = 0)$ on the detector as the intercept of the specular scattering plane with that of the crystal surface.

Figure 1 displays intensity plots of the scattering profiles for collision of 200 eV He atoms on a LiF(001) surface for the beam aligned along the [110] and [100] directions. Both profiles reveal discrete spots distributed on the circle of constant normal energy:

$$p_y^2/2M + p_z^2/2M = E_\perp = E_0\sin^2\theta. \qquad (1)$$

Here E_0 is the total projectile energy, and $p_y(p_z)$ stands for momentum along $y(z)$ axis. The projections show that the spots are regularly spaced in the y direction parallel to the surface plane. This is attributed to the diffraction of the scattered beam by the periodic surface potential.

The important feature is that, for a given surface orientation the observed spacing between spots does not depend on the angle of incidence θ but only on the de Broglie wavelength λ of the projectile. This is shown in Fig. 2 for different atomic and molecular projectiles with energies up to 2.5 keV colliding on both LiF(001) and NaCl(001) surfaces. The beam alignment is along the [110] and [100] directions. The reciprocal lattice vectors $\mathbf{G}_1$ and $\mathbf{G}_2$ are aligned along [110] and [1$\bar{1}$0] directions, respectively (see Fig. 1 and 2). For the [110] direction of the scattered beam one of the reciprocal lattice vectors is along the y axis. Therefore, the experimental result $\Delta p_y/G = 1$ clearly confirms that the observed features in the scattering profile are due to the diffraction of the incident beam at the surface (unless otherwise stated, atomic units are used). The situation is different for the [100] direction of the scattered beam where experimental data show $\Delta p_y/G = $

$\sqrt{2}$ which is twice larger than what one would expect if only one reciprocal lattice vector is exchanged between the projectile and the lattice.

The experimental observations can be understood within the semiclassical approach. Taking into account (i) the high beam energy where the particle wavelength is much smaller than the amplitude of the thermal vibrations of the lattice atoms, and (ii) grazing scattering geometry, we write the projectile wave function as

$$\Psi(x, y, z) = \psi(y, z)e^{ip_x x}, \qquad (2)$$

where the motion along the x coordinate is fast and proceeds with constant momentum $p_x = \sqrt{2ME_0\cos^2\theta}$. The motion in the (yz) plane is slow and corresponds to the energy $E_\perp = E_0\sin^2\theta$ and an associated wavelength $\lambda_\perp = \lambda/\sin\theta \approx \lambda/\theta$. The periodic surface scattering potential can be represented as

$$V(x, y, z) = \sum_{j_1,j_2}V_{j_1,j_2}(z)e^{i(j_1\mathbf{G}_1 + j_2\mathbf{G}_2)(\hat{e}_x x + \hat{e}_y y)}, \qquad (3)$$

with $\hat{e}_{x(y)}$ unit vectors in $x(y)$ direction. For the wave function given by Eq. (2), the only potential matrix elements that cause the transitions correspond to $V_{n,m}(z)$ where the pair (n, m) verifies: $(n\mathbf{G}_1 + m\mathbf{G}_2)\hat{e}_x = 0$. The potential structure in the direction of the incident beam is not resolved, and the projectile only exchanges a combination of the reciprocal lattice vectors pointing in the direction y perpendicular to the classical (xz) specular scattering plane. This corresponds to the intuitive picture, where, seen from grazing incidence, the surface is not made of atoms but of structureless parallel furrows aligned
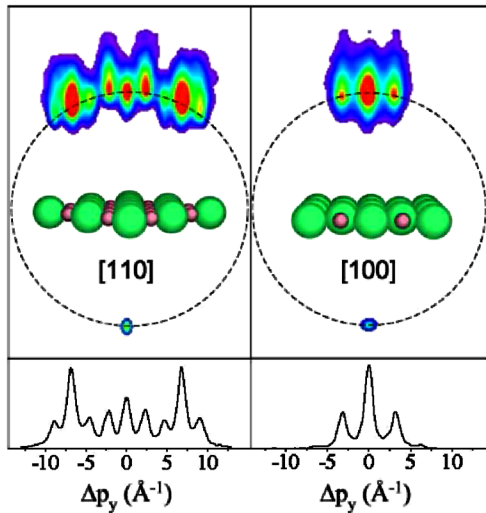

FIG. 1 (color online).   Diffraction patterns of 200 eV He atoms scattered on LiF(001) surface aligned along the [110] (left) and [100] (right) direction. The image corresponds to the (yz) plane and the tiny spot in the bottom is from projectiles that did not hit the target. The dashed circles indicate a constant normal energy [Eq. (1)]; its radius corresponds to 1.5°, the angle of incidence. The 1D profiles in the bottom are the projections on the y axis (horizontal direction) of the scattering profiles. The insets show the surface orientation relative to the beam direction.
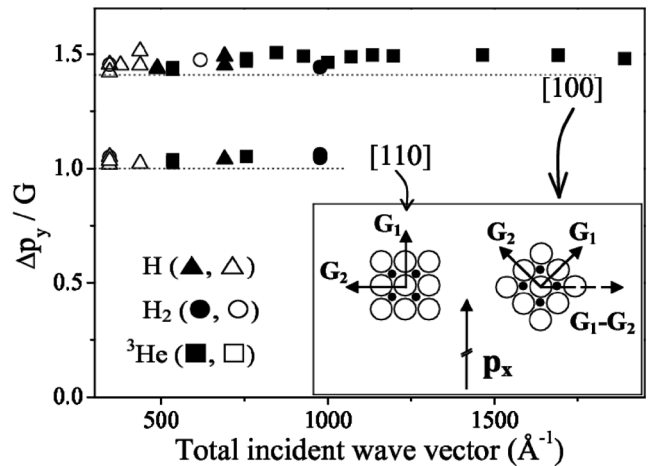

FIG. 2.   For various projectiles colliding at different energies and incidence angles on LiF (filled symbols) and NaCl (hollow symbols), the spacing Δy between adjacent diffraction spots is plotted as a momentum exchanged Δp_y expressed in units of the target reciprocal vector $G = 2\sqrt{2}\pi/a$, where $a = 4.03(5.64)$ Å is the LiF (NaCl) lattice constant. The apparent symmetry depends only on the crystal azimuthal orientation. The inset sketches the orientation of the lattice and its reciprocal lattice vectors G_1 and G_2 relative to the beam (p_x).

along the observation direction. The system possesses the translational symmetry along the direction of observation and the proper 1D lattice unit is then the spacing between identical furrows. The diffraction proceeds in the (yz) plane and is driven by the effective potential resulting from the averaging of the actual 3D surface potential along the x direction

$$V_{2D}(y, z) = \sum_{(n,m)} V_{n,m}(z) e^{i(n\mathbf{G}_1 + m\mathbf{G}_2)\hat{e}_y y}. \quad (4)$$

The momentum of the diffracted particles in the y direction is given by: $p_y = (n\mathbf{G}_1 + m\mathbf{G}_2)\hat{e}_y$, and the corresponding momentum perpendicular to the surface, p_z, can be deduced from the energy conservation [Eq. (1)]. Observe that the pertinent wavelength is the one associated with slow motion perpendicular to the surface, $\lambda_\perp$. It is comparable to the spacing between furrows allowing for diffraction.

A full quantum mechanical treatment with a *perfectly* periodic surface leads to the same results (see below) confirming this semiclassical approach. Indeed, consider the scattering from the perfectly periodic surface within the frame moving along x direction with velocity $v = p_x/M$. The potential given by Eq. (3) depends on time through the substitution $x \rightarrow x + vt$. Exchange of the momentum with the lattice $\Delta\mathbf{p} = j_1\mathbf{G}_1 + j_2\mathbf{G}_2$ is associated to the energy change $\Delta E = (\Delta\mathbf{p})^2/2M$ while the corresponding matrix element oscillates with the frequency $\omega = \Delta\mathbf{p}\hat{e}_x v$. For a fast projectile, $\omega \gg \Delta E$ and transitions are only possible for the pairs $(j_1 = n, j_2 = m)$ such that $\Delta\mathbf{p}\hat{e}_x = 0$. Thus, diffraction proceeds in the (yz) plane, and p_x is preserved. Similar effect, i.e., progressive attenuation of the in-plane scattering intensity when approaching grazing incidence, has been reported by Farias *et al.* [14] for the scattering of thermal H_2 projectiles.

Now, we return to the discussion of Fig. 2. Obviously, for the incident beam oriented along [110] direction, the y axis is parallel to $\mathbf{G}_2$ so that all pairs $(0, m)$ are possible. This leads to $|p_y| = |m|G$ and the spacing between adjacent spots equal to G. For the incident beam oriented along [100] direction only combinations $(m, -m)$ are possible, and $|p_y| = |m|\sqrt{2}G$ with spacing between adjacent spots given by $\sqrt{2}G$. One can also use the intuitive picture, where adjacent rows along the [100] direction consist of alternating alkali and halide ions. The furrows are separated by half a lattice constant leading to the "effective" reciprocal lattice vector of length $4\pi/a = \sqrt{2}G$. At variance, along the [110] direction the periodicity of the alkali and halide furrows is given by G. To summarize this geometric aspect, the observed diffraction corresponds exclusively to exchange of reciprocal vectors perpendicular to the beam direction (along y) while the observed periodicity is the spacing between equivalent furrows. Importantly, the latter is not necessarily equivalent to the real period of the surface structure.

We have used the wave packet propagation approach to calculate the ^3He atom scattering from the LiF(001) sur-

face. The methodology employed here is similar to the well-documented quantum treatments of low-energy molecular scattering from surfaces [15]. In brief, the time dependent Schrödinger equation is solved for the initial wave function corresponding to the Gaussian wave packet in z-coordinate incident at the surface $\psi(t = 0) = e^{ip_x x} e^{-i\alpha z - (z-z_0)^2/\sigma^2}$. The time propagation is done with Fourier grid pseudospectral approach [16] allowing easy incorporation of the periodicity of the system. The scattering matrix is then extracted within the $E_\perp = p_z^2/2M$ range covered by initial state. The ground state potential energy surface for He/LiF(001) scattering was determined using the quantum chemistry HONDO7 program [17]. The actual calculations use the F_5Li_5 and F_4Li_5 clusters embedded in the point charge lattice [18].

Figure 3 presents the calculated and measured intensities of the diffraction orders as a function of the normal energy component $E_\perp$ for a beam energy of $E_0 = 200$ eV. The agreement between theory and experiment is quite satisfactory supporting our interpretation in terms of quantum diffraction. As seen in Fig. 3 the higher diffraction orders can be only observed at larger angles of incidence (larger $E_\perp$). Indeed, energy conservation in Eq. (1) gives a threshold $p_y^2/2M = E_\perp$ corresponding to a diffraction in the surface plane ($p_z = 0$). More interesting is that the relative intensities associated with each diffraction order vary rapidly with $E_\perp$ showing pronounced oscillations. Following basic interpretation developed in TEAS, oscillating structure can be qualitatively understood in a semiclassical picture as due to interferences between different trajectories bouncing on top and between the atomic rows. This can be turned quantitative when the 2D averaged potential (with translational symmetry along the beam axis x) is replaced by a hard corrugated wall model of the surface.
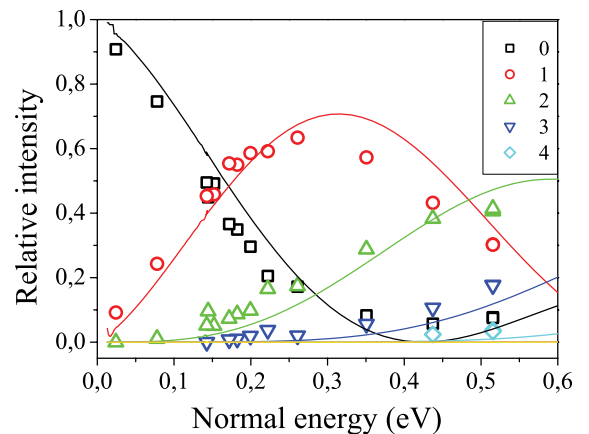

FIG. 3 (color online). For 200 eV He atoms scattered on LiF(001) surface aligned along the [100] direction, the figure reports the evolution of the relative intensities of the observed diffraction orders with the normal energy, i.e., with the angle of incidence θ. Symbols stand for the experimental data and solid lines show the results of the wave packet propagation described in the text.

The position of the infinite repulsive wall given by: $z = z_c \cos(2\pi y/b)$, b being the distance between equivalent furrows. The intensity I_m of the diffraction order m is then given by $I_m = J_m^2(2\alpha)$ [19], where $J_m(2\alpha)$ is the Bessel function of rank m and $\alpha = 2\pi z_c/\lambda_\perp$ is a dimensionless measure of the corrugation. With this free corrugation parameter z_c, this simple model reasonably reproduces the results presented in Fig. 3 allowing a straightforward interpretation in terms of a smooth monotonic evolution of the corrugation $z_c(E_\perp)$.

We have demonstrated that keV projectiles can be diffracted by the periodic surface potential, thus showing quantum behavior. The results presented here correspond to a new regime of atomic diffraction on crystal surfaces. Neglecting thermal vibrations, the diffraction pattern may be understood as deriving from the interaction at normal incidence of a particle of energy $E_\perp$ on a periodic 2D potential [Eq. (4)]. In this respect, this is a projection technique only sensitive to the average of the actual 3D surface potential along the direction of the incident beam. By analogy with the well-established TEAS technique, the interferometric nature of the measurements suggests that this 2D potential may be derived with a high accuracy. For the present system, diffraction is observed for $E_\perp$ ranging from 10 meV up to almost 1 eV so that this new technique nicely complements TEAS, including the most recent low temperature developments where μeV [20] and neV [21] resolution have been demonstrated for beam energies in the meV range. The grazing incidence geometry together with the comparatively high energy of the projectiles in the keV range allows the full diffraction pattern to be recorded at once onto a position sensitive detector. The detection scheme is then comparable to that used in reflection high energy electrons (RHEED) diagnostics that have proved successful for *online* monitoring of molecular beam epitaxy. More work is needed to explore the line shape and the various sources of decoherence. The thermal vibrations of the surface atoms are partly washed out by the finite averaging along the beam direction so that on LiF, diffraction is well observed even at 1000 K calling for a modified Debye-Waller factor [22]. The influence of various electronic excitations can be investigated by energy loss measurements on different target materials such as semiconductors and metals. The role of the internal degrees of freedom of molecular projectiles on the coherence appears also of great interest. More prospective, Fig. 3 shows that at normal energy $E_\perp = 0.25$ eV, the surface can act as an efficient beam splitter with more than half of the beam scattered in the ± 1 diffraction order. This opens the possibility of atoms optics in the keV range keeping in mind that coherence exists only in the transverse direction.

*Electronic address: roncin@lcam.u-psud.fr

[1] I. Estermann and O. Stern, Z. Phys. **61**, 95 (1930).
[2] A. Graham, Surf. Sci. Rep. **49**, 115 (2003).
[3] G. Witte, J. Braun, A. Lock, and J. P. Toennies, Phys. Rev. B **52**, 2165 (1995).
[4] M. A. Van Hove, W. H. Weinberg, and C.-M. Chan, *Low-Energy Electron Diffraction* (Springer-Verlag, Berlin, 1986).
[5] T. A. Pasquini, Y. Shin, C. Sanner, M. Saba, A. Schirotzek, D. E. Pritchard, and W. Ketterle, Phys. Rev. Lett. **93**, 223201 (2004).
[6] J. Baudon, R. Mathevet, and J. Robert, J. Phys. B **32**, R173 (1999).
[7] *Atom Interferometry*, edited by P. Berman (Academic, New York, 1997).
[8] *Principles and Applications of Ion Scattering Spectroscopy*, edited by J. W. Rabalais (Wiley-Interscience, New York, 2003).
[9] H. Winter, Phys. Rep. **367**, 387 (2002).
[10] V. Ignatova, D. Karpuzov, I. Chakarov, and I. Katardjiev Prog. Surf. Sci. **81**, 247 (2006); J. F. Ziegler, J. P. Biersack, and U. Littmark, *The Stopping and Range of Ions in Solids* (Pergamon, New York, 1985).
[11] L. Folkerts, S. Schippers, D. M. Zehner, and F. W. Meyer, Phys. Rev. Lett. **74**, 2204 (1995).
[12] A. Schüller, G. Adamov, S. Wethekam, K. Maass, A. Mertens, and H. Winter, Phys. Rev. A **69**, 050901(R) (2004).
[13] P. Roncin, J. Villette, J. P. Atanas, and H. Khemliche, Phys. Rev. Lett. **83**, 864 (1999).
[14] D. Farias, C. Diaz, P. Riviere, H. F. Busnengo, P. Nieto, M. F. Somers, G. J. Kroes, A. Salin, and F. Martin, Phys. Rev. Lett. **93**, 246104 (2004); D. Farias, C. Diaz, P. Nieto, A. Salin, and F. Martin, Chem. Phys. Lett. **390**, 250 (2004).
[15] P. Nieto, E. Pijper, D. Barredo, G. Laurent, R. A. Olsen, E-J. Baerends, G.-Jan. Kroes, and D. Farías, Science **312**, 86 (2006).
[16] R. Kosloff, J. Phys. Chem. **92**, 2087 (1988).
[17] M. Dupuis, J. D. Watts, H. O. Villar, and G. J. B. Hurst, Comput. Phys. Commun. **52**, 415 (1989).
[18] A. G. Borisov, J. P. Gauyacq, V. Sidis, and A. K. Kazansky, Phys. Rev. B **63**, 045407 (2001).
[19] R. I. Masel, R. P. Merrill, and W. H. Miller, Phys. Rev. B **12**, 5545 (1975).
[20] A. P. Jardine, S. Dworski, P. Fouquet, G. Alexandrowicz, D. J. Riley, G. Y. H. Lee, J. Ellis, and W. Allison, Science **304**, 1790 (2004).
[21] M. DeKieviet, D. Dubbers, C. Schmidt, D. Scholz, and U. Spinola, Phys. Rev. Lett. **75**, 1919 (1995).
[22] G. Armand and J. R. Manson, Phys. Rev. Lett. **53**, 1112 (1984).